

## REPORTS

## PLANETARY DYNAMICS

# A class of warm Jupiters with mutually inclined, apsidally misaligned close friends

Rebekah I. Dawson\* and Eugene Chiang

The orbits of giant extrasolar planets often have surprisingly small semimajor axes, large eccentricities, or severe misalignments between their orbit normals and their host stars' spin axes. In some formation scenarios invoking Kozai-Lidov oscillations, an external planetary companion drives a planet onto an orbit having these properties. The mutual inclinations for Kozai-Lidov oscillations can be large and have not been confirmed observationally. Here we present evidence that observed eccentric warm Jupiters with eccentric giant companions have mutual inclinations that oscillate between 35° and 65°. Our inference is based on the pairs' observed apsidal separations, which cluster near 90°. The near-orthogonality of periape directions is effected by the outer companion's quadrupolar and octupolar potentials. These systems may be undergoing a stalled version of tidal migration that produces warm Jupiters over hot Jupiters, and they provide evidence for a population of multiplanet systems that are not flat and have been sculpted by Kozai-Lidov oscillations.

Planet-planet scattering (1), secular chaos (2), and Kozai-Lidov oscillations (3, 4) induced by a stellar (5) or planetary (6) perturber are each capable of exciting the eccentricities of giant planets (7, 8), of shrinking orbits by tidal friction to form close-in hot Jupiters [having semimajor axes  $a < 0.1$  astronomical unit (AU)], and of tilting hot Jupiters' orbit normals away from their host stars' spin axes (9–14).

There are two outstanding issues with these models. First, they require or produce large inclinations between planetary orbits. These have not yet been observed. Most of the few systems with measured mutual inclinations are composed of planets on coplanar, low-eccentricity, mean-motion resonant orbits, such as GJ 876 (15) and Kepler-30 (16). This breed of system is thought to result from gentle disk migration (17), not from Kozai oscillations, planet scattering, or secular chaos. The two exceptions contain well-spaced (i.e., nonresonant) giant planets. Based on astrometry with the Hubble Space Telescope fine guidance sensor, a mutual inclination of 30° between Upsilon Andromeda c and d was inferred (18). From transit timing variations, a mutual inclination of  $9^{+8}_{-6}$  between Kepler-419 (KOI-1474) b and c was measured (19).

The second problem is that current models do not easily produce warm Jupiters, located exterior to hot Jupiters but interior to the pileup of giant planets at 1 AU (20). Although intrinsically rare, warm Jupiters promise to distinguish among models by serving as the exception that proves the

rule. Many warm Jupiters have present-day eccentricities too high to have resulted from planet-planet scattering, because giant planets at small

orbital distances collide and circularize before their velocity dispersions become too elevated (21). Yet most of their observed eccentricities are also too low to be easily accommodated within formation scenarios for hot Jupiters that invoke tidal migration (22), because warm Jupiters' current periapees are too far from their host stars for tidal friction to operate effectively.

One possibility (23) is that eccentric warm Jupiters are undergoing “slow Kozai” (24) migration driven by an external, mutually inclined companion. In this interpretation, warm Jupiters are observed today at the low-eccentricity phases of their secular Kozai cycles and only rarely attain eccentricities high enough for tidal friction to operate. For Kozai oscillations to not be quenched at these small semimajor axes by general relativistic precession, the external perturber must be nearby: It must be a “close friend” (23), in contrast to a “cold friend” (25). Supporting the possibility of migration driven by close friends, eccentric warm Jupiters orbit stars more enriched in metals—and therefore more likely to host multiple giant planets—than those of their circular counterparts (26). Indeed, the warm Jupiters known to have external giant planetary companions exhibit a broader range of eccentricities than solitary warm Jupiters (23). A key question is whether the mutual orbital inclination  $i_{\text{mut}}$  between warm Jupiters and their exterior companions exceeds 39.2°, the minimum angle required to excite Kozai oscillations in the quadrupole approximation (3, 4). Unfortunately, nearly all of these planets are detected by

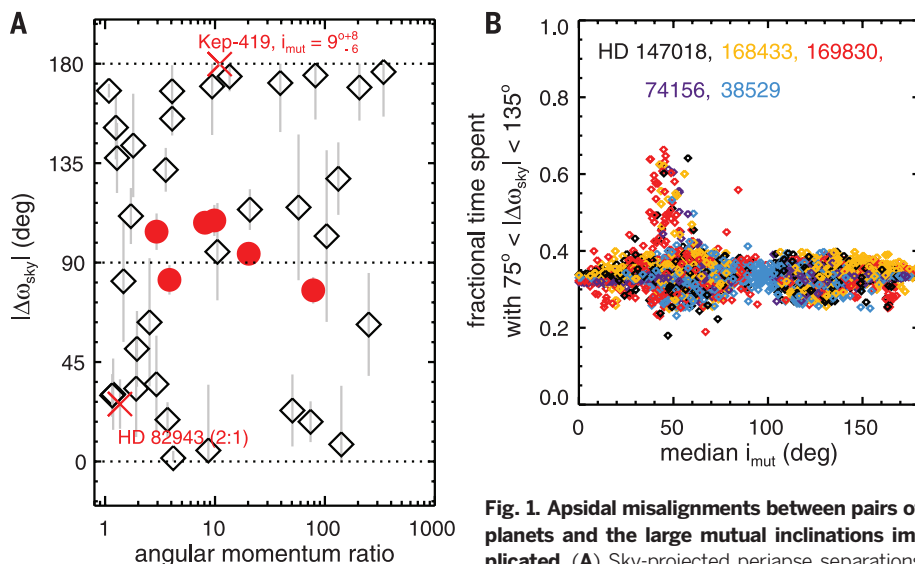


**Fig. 1. Apsidal misalignments between pairs of planets and the large mutual inclinations implicated.** (A) Sky-projected periape separations

$|\Delta\omega_{\text{sky}}|$  of planetary pairs, where  $-180^\circ < |\Delta\omega_{\text{sky}}| < 180^\circ$ . The sample includes all RV- and transit-discovered pairs with well-constrained (30) eccentricities and arguments of periape. No mass or semimajor axis cut is made on the black diamonds. The red circles (corresponding to systems shown also in Figs. 2 and 3 and figs. S1 to S5) and crosses (HD 82943 and Kepler-419) represent warm Jupiters with only one known companion beyond 1 AU. All six of the red circles (51) lie close to  $|\Delta\omega_{\text{sky}}| = 90^\circ$ ; i.e., their apsides are strongly misaligned. For calculation of the abscissa values, the orbital angular momentum is evaluated as  $m \sin i_{\text{sky}} \sqrt{a(1-e^2)}$ . (B) Fraction of time that  $|\Delta\omega_{\text{sky}}|$  spends near  $90^\circ$ , as a function of median mutual inclination, for stable simulations of systems corresponding to five of the six red circles (the same five are shown in Fig. 2). HD 202206 is omitted; its architecture and apsidal behavior differ from those of the five (fig. S5). Each simulation is consistent with the observed orbital elements, but only those with  $i_{\text{mut}}$  near  $40^\circ$  spend extra time at  $|\Delta\omega_{\text{sky}}| \sim 90^\circ$ . The fractional time is evaluated for  $75^\circ < |\Delta\omega_{\text{sky}}| < 135^\circ$ ; this window is centered on  $105^\circ$  instead of  $90^\circ$  because of general-relativistic precession.

Department of Astronomy, University of California, Berkeley, Hearst Field Annex 3411, Berkeley, CA 94720-3411, USA.

\*Corresponding author. E-mail: rdawson@berkeley.edu

**EMBARGOED UNTIL 2PM U.S. EASTERN TIME ON THE THURSDAY BEFORE THIS DATE:**

the radial velocity (RV) method, which does not yield  $i_{\text{mut}}$  directly but instead measures a given planet's  $a$ , eccentricity  $e$ , minimum mass  $m \sin i_{\text{sky}}$  (where  $i_{\text{sky}}$  is the orbital inclination with respect to the sky plane), and argument of periape  $\omega_{\text{sky}}$  (referred to the sky plane).

However, the sky-projected apsidal separation of a planetary pair,  $\Delta\omega_{\text{sky}}$ , can be a clue to  $i_{\text{mut}}$  (27). In the invariable plane, the difference in apsidal longitudes  $\Delta\omega_{\text{inv}}$  (for which  $\Delta\omega_{\text{sky}}$  is our observable proxy) is often found near  $0^\circ$  or  $180^\circ$  for pairs of coplanar planets, either in the secular limit (28) or in the 2:1 mean-motion resonance (17). In contrast, for highly inclined systems there is no such preference to find  $\Delta\omega_{\text{inv}}$  near  $0^\circ$  or  $180^\circ$ , at least for secular systems (27). The behavior of  $\Delta\omega_{\text{inv}}$  is directly reflected by its projection  $\Delta\omega_{\text{sky}}$ . Figure 1A displays  $|\Delta\omega_{\text{sky}}|$  for RV-detected planetary pairs (29), some of which include warm Jupiters but most of which do not, with well-

constrained (30)  $e$  and  $\omega_{\text{sky}}$ , as a function of angular momentum ratio. Most systems with angular momentum ratio  $> \sim 3$  have  $|\Delta\omega_{\text{sky}}|$  near  $0^\circ$  and  $180^\circ$ . But some pairs with similarly large ratios are clustered near  $90^\circ$ .

The cluster of systems having  $|\Delta\omega_{\text{sky}}| \sim 90^\circ$  includes eccentric warm Jupiters with eccentric close friends. In fact, if we turn the problem around and consider only those systems with eccentric pairs consisting of one warm ( $0.1 < a < 1$  AU) and one “balmy” ( $a > 1$  AU) Jupiter (defined as  $m \sin i_{\text{sky}} > 0.1 M_{\text{Jupiter}}$ ) without regard for  $|\Delta\omega_{\text{sky}}|$ , then of the eight systems (31) so selected (red symbols in Fig. 1A), six (red circles) have  $|\Delta\omega_{\text{sky}}|$  near  $90^\circ$  (HD 147018, HD 38529, HD 168443, HD 74156, HD 169830, and HD 202206). The two systems we know or expect to have low mutual inclinations (red crosses) are not among these six pairs with  $|\Delta\omega_{\text{sky}}|$  clustered near  $90^\circ$ . HD 82943 (bottom red cross) is li-

brating in the 2:1 mean-motion resonance (32), which interferes with the purely secular interactions we studied by driving apsidal precession on a shorter, resonant time scale. Another outlier is the transit-detected system Kepler-419 (top red cross), which was recently found to host an eccentric pair of one warm and one balmy Jupiter having a low ( $9^\circ \pm 5^\circ$ ) mutual inclination and an apsidal separation of  $|\Delta\omega_{\text{sky}}| = 179.8^{+0.6}_{-0.7} (19)$ . The orbital elements of all eight systems are listed in table S1.

Here we argue that the  $\sim 90^\circ$  apsidal misalignment between warm Jupiters and their close friends signifies a mutual inclination of  $\sim 40^\circ$ , just above the lower limit for Kozai oscillations. For each of the six systems identified above (33), we performed  $\sim 1000$  numerical orbit integrations, starting with initial conditions that randomly assign the two angles not constrained by the radial-velocity data,  $i_{\text{sky}}$  and  $\Omega_{\text{sky}}$ , the latter being the longitude of the ascending node on the sky plane (with the mass  $m$  chosen to satisfy the measured  $m \sin i_{\text{sky}}$ ). These angles are drawn (independently for each planet) from a uniform distribution spanning  $-1 < \cos i_{\text{sky}} < 1$  and  $0^\circ < \Omega_{\text{sky}} < 360^\circ$ , resulting in an isotropic distribution of orbits. For an additional 180 simulations, we fixed  $i_{\text{sky},1} = i_{\text{sky},2} = 90^\circ$  and  $\Omega_{\text{sky},2} = 0^\circ$ , and drew  $\Omega_{\text{sky},1}$  from a uniform distribution spanning  $0^\circ$  to  $180^\circ$ . The eccentricities, semimajor axes, mean anomalies, and  $\omega_{\text{sky}}$ 's are set to those observed. All numerical integrations in this paper used the  $N$ -body code Mercury6 (34), with the Bulirsch-Stoer integrator (bs) modified to include general-relativistic precession (35).

In Fig. 1B, we plotted the fraction of time that each simulated stable system spends having  $75^\circ < |\Delta\omega_{\text{sky}}| < 135^\circ$ , as a function of median mutual inclination, for five of our six systems (the sixth is a special case discussed below). A separation of  $\Delta\omega_{\text{sky}} = 270^\circ = -90^\circ$  is equivalent to  $90^\circ$  in that both yield  $|\Delta\omega_{\text{sky}}| = 90^\circ$ . Each simulation was inspected by eye to ensure that the integration duration was long enough to sample the behavior of  $\Delta\omega_{\text{sky}}$ ; integration durations range from 0.15 to 100 million years. A similar exploration of parameter space (36) was performed for two of our systems, HD 38529 and HD 168443, but without our aim of identifying regions of parameter space where  $|\Delta\omega_{\text{sky}}|$  lingers near  $90^\circ$ . As illustrated in Fig. 1B, in the five systems we encounter configurations in which  $|\Delta\omega_{\text{sky}}|$  spends excess time near  $90^\circ$ , but only for median  $i_{\text{mut}} \sim 39^\circ$ , near Kozai's critical inclination. For such systems,  $|\Delta\omega_{\text{sky}}|$  spends one-half to two-thirds of the time between  $75^\circ$  and  $135^\circ$ , depending on initial conditions. In comparison, uniform circulation of  $|\Delta\omega_{\text{sky}}|$  gives a fractional time of one-third. Nearly coplanar systems for which  $|\Delta\omega_{\text{sky}}|$  librates about  $0^\circ$  or  $180^\circ$  may spend no time at all in the desired range. Such realizations are inconsistent with the radial-velocity data and accordingly do not appear in Fig. 1B. The sixth system, HD 202206, is distinctive because its warm Jupiter is much more massive than the outer companion and because it lies near the 5:1 resonance. For this system, we still encounter configurations with  $i_{\text{mut}} \sim 40^\circ$  that

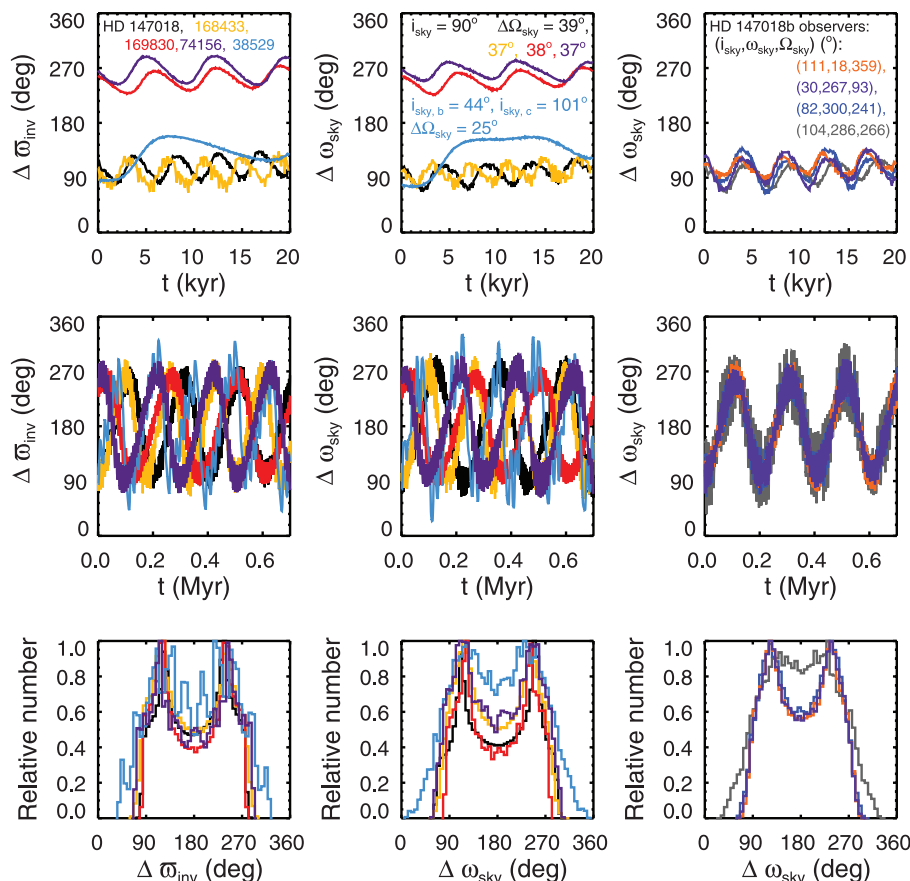


**Fig. 2. Sample time histories of apsidal misalignment for five planetary pairs of warm Jupiters and their outer companions. Initial conditions are taken from table S1, with additional orbital angles indicated in the legend.** For every history shown, the mutual inclination between the pair of planets varies within an interval that does not fall outside of  $35^\circ$  to  $65^\circ$ . (Top) On short time scales, the apsidal separation lingers near  $90^\circ$  or  $270^\circ$ . (Middle) Over longer time scales, the apsidal misalignment librates about  $180^\circ$  with an amplitude of  $90^\circ$ . (Bottom) Relative occurrence of either the apsidal separation evaluated in the invariable plane ( $\Delta\omega_{\text{inv}}$ ) or the sky-projected apsidal separation ( $\Delta\omega_{\text{sky}}$ ), in uniformly spaced bins, indicating that these angles spend excess time near  $90^\circ$  and  $270^\circ$ . Because of the lower oscillation frequencies characterizing HD 38529 and HD 74156, for these two systems we plotted  $t/3$  as the abscissa in both top and middle rows. Unlike the systems shown here, HD 202206 is situated near the 5:1 resonance, and its inner planet is almost certainly more massive than its outer planet (table S1); its dynamics is explored in fig. S5.



spend excess time with  $|\Delta\omega_{\text{sky}}|$  near  $90^\circ$ , but not in the conventional range of  $75^\circ$  to  $135^\circ$ . An example is shown in fig. S5.

We reiterate that those integrations exhibiting libration of  $|\Delta\omega_{\text{sky}}|$  about  $90^\circ$  all have  $i_{\text{mut}}$  close to  $39.2^\circ$ ; typically,  $i_{\text{mut}}$  varies within an interval that does not fall outside  $35^\circ$  to  $65^\circ$  over the course of a given integration. In contrast, nearly coplanar, polar, or retrograde configurations consistent with the radial-velocity data have  $|\Delta\omega_{\text{sky}}|$  circulating in the integrations we performed. Figure 2 shows examples of how the apsidal separation lingers near  $90^\circ$  and  $270^\circ$ , in the sky plane and invariable plane, over many

secular oscillations. The desired libration of  $|\Delta\omega_{\text{sky}}|$  does not require a finely tuned viewing geometry or set of initial conditions. Regarding viewing geometry, the libration of  $|\Delta\omega_{\text{sky}}|$  is similar to that of  $|\Delta\omega_{\text{inv}}|$  for most observer orientations. Taking a single integration of HD 147018 for which  $|\Delta\omega_{\text{inv}}|$  spends 60% of its time between  $75^\circ$  and  $135^\circ$  in the invariable plane, we viewed this system from the vantage points of 500 isotropically distributed observers. We find that 60% (80%) of observers measure  $75^\circ < |\Delta\omega_{\text{sky}}| < 135^\circ$  at least 50% (40%) of the time. Measurements from four example observers are given in the right column of Fig. 2. Regarding initial conditions, we numerically

integrated different realizations of the five systems shown in Fig. 2, ignoring all observational constraints on  $\omega_{\text{sky}}$  and starting from various combinations of initial  $\{\omega_{\text{inv},1}, \omega_{\text{inv},2}, i_{\text{mut}}\}$ , with  $35^\circ < i_{\text{mut}} < 65^\circ$ . To simplify and speed up these calculations, we approximated the inner planet as a test particle and integrated the secular equations of motion. Among the many realizations thus constructed (three are shown in fig. S6 along with accompanying surfaces of section), we find that it is not unusual for  $\Delta\omega_{\text{inv}}$  (and by extension  $\Delta\omega_{\text{sky}}$ ) to linger near  $90^\circ/270^\circ$ ; i.e., it is not uncommon for  $\Delta\omega_{\text{inv}}$  to librate about  $180^\circ$  with a libration amplitude of  $90^\circ$ . Actually, depending on initial conditions,  $\Delta\omega_{\text{inv}}$  can librate about either  $180^\circ$  or  $0^\circ$  with a variety of amplitudes, as well as circulate, and we discuss later why warm Jupiters may prefer a libration amplitude near  $90^\circ$ .

The apsidal libration we observed has been seen in other celestial mechanical contexts; it is qualitatively similar to the “artichoke-shaped” (37) libration exhibited by Saturn’s irregular satellites Narvi (38) and, for some initial conditions, Pasiphae (37, 39). Both Narvi and Pasiphae orbit Saturn with inclinations of  $\sim 140^\circ$  with respect to the plane of Saturn’s orbit about the Sun. In the context of triple stellar systems, “beatlike” patterns with superposed short- and long-time scale oscillations, similar to those shown in Fig. 2, were noticed in the modeled eccentricity variations of systems with  $i_{\text{mut}} \sim 40^\circ$  and attributed to interference between the quadrupolar and octupolar potentials (40). The configurations of interest here do not lie near any border between circulation and libration; i.e.,  $\Delta\omega_{\text{inv}}$  librates about  $180^\circ$  with an amplitude of  $90^\circ$ , not  $180^\circ$ . In particular, the dynamics responsible for how  $|\Delta\omega_{\text{inv}}|$  lingers near  $90^\circ$  is dissimilar from the “borderline” behavior of nearly coplanar systems in which  $|\Delta\omega_{\text{inv}}|$  speeds through  $180^\circ$  but does not linger near  $90^\circ$  (41, 42).

We can reproduce the observed libration of  $\Delta\omega_{\text{inv}}$  by approximating a warm Jupiter as a test particle perturbed by an exterior body and solving Lagrange’s equations of motion using a secular disturbing potential expanded to octupolar order (39), including general-relativistic precession of both planets’ orbits (35). The octupolar potential plays an essential role in generating a precession rate  $d\Delta\omega_{\text{inv}}/dt$  that cancels, on average, the precession rate induced by the quadrupolar potential; the net result is that  $\Delta\omega_{\text{inv}}$  librates. Therefore, the perturber must not only be near enough to dominate general-relativistic precession (5, 23) but must also be eccentric. The strength of the octupolar potential is proportional to the perturber’s eccentricity. The importance of the octupolar potential has only recently been recognized in the exoplanet literature (6, 40). A popular application has been to flip an interior body from a prograde to retrograde orbit at large eccentricities (6, 43, 44, 45–47). A low mutual inclination, well below Kozai’s critical angle, is sufficient to spur such a flip if the inner planet’s eccentricity is high enough (46, 47). The regime explored

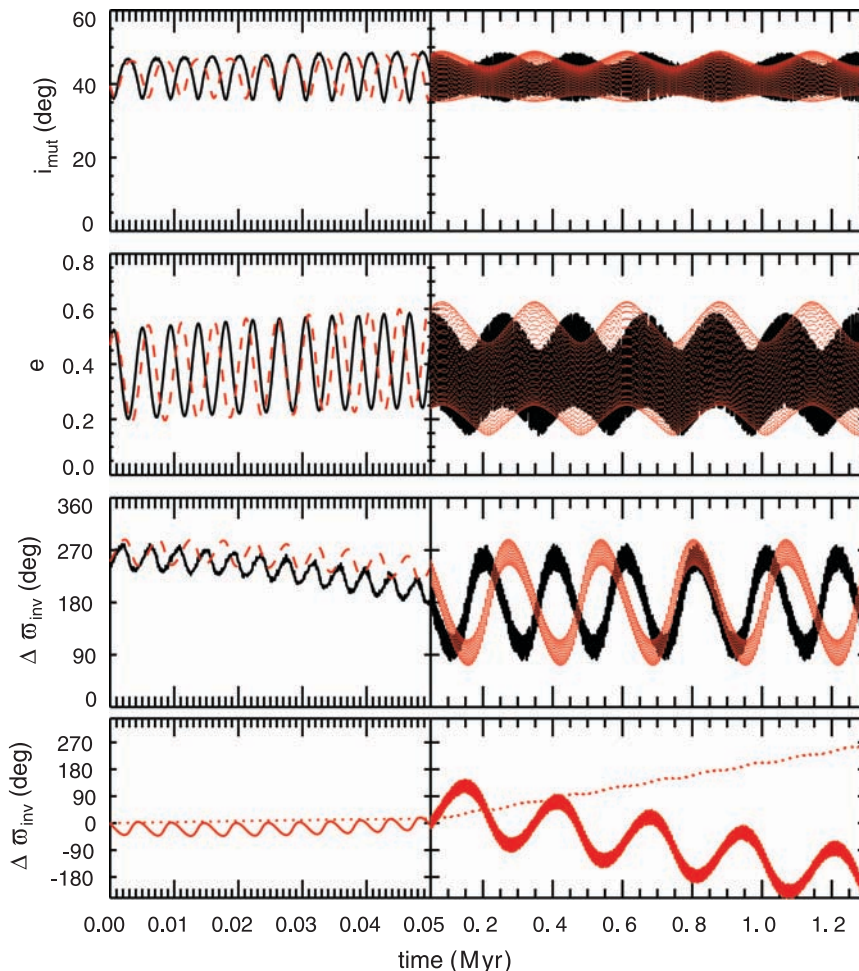


**Fig. 3. Orbital evolution of HD 147018b, calculated using an  $N$ -body simulation and using a secular Hamiltonian expanded to octupolar order.** Plotted are the time evolution of the mutual inclination (row 1), eccentricity of the inner warm Jupiter (row 2), apsidal separation (row 3), and near-canceling contributions to the apsidal separation from the quadrupolar and octupolar potentials (row 4). The simulation was performed in the invariable plane. Initial conditions were for the HD 147018 system (table S1) with  $i_{\text{sky}} = 90^\circ$  and  $\Delta\omega_{\text{sky}} = 39^\circ$ , corresponding to  $i_{\text{mut}} = 39^\circ$  and to angles  $\{i_1 = 35.6^\circ, \omega_1 = 66.0^\circ, \Omega_1 = 0^\circ\}$  and  $\{i_2 = 3.4^\circ, \omega_2 = 136.9^\circ, \Omega_2 = 180^\circ\}$  in the invariable plane. All black curves in this figure are taken from the same Mercury6  $N$ -body integration underlying the black curves in the left column of Fig. 2. Red curves are for a test particle integrated using Lagrange’s equations of motion for the octupolar Hamiltonian (39). The bottom row is computed by separating the Hamiltonian into the quadrupolar terms (dotted line) and octupolar plus general-relativistic terms (solid line); by evaluating their respective contributions to  $\dot{\omega}_1$  using Lagrange’s equations of motion; and by integrating  $\dot{\omega}_1$ , setting the constant of integration to zero for simplicity. (The quantities  $e$  and  $i_{\text{mut}}$  are computed from the full Hamiltonian.) The sum of the dotted and solid curves in the bottom row equals the deviation of the red curve in the third row from its initial value. The secular behavior of the test particle reproduces qualitatively well that of the full  $N$ -body integration.

here, which produces warm Jupiters with the observed clustering of  $|\Delta\omega_{\text{sky}}|$  near  $90^\circ$ , is complementary: Both the inner and outer planets' eccentricities are too modest for the octupolar potential to effect flips, and  $i_{\text{mut}}$  remains near  $40^\circ$ , a prograde configuration. We deduced that our six systems with warm Jupiters and close friends are prograde, with  $i_{\text{mut}} \sim 40^\circ$  rather than retrograde with  $i_{\text{mut}} \sim 140^\circ$ , because in the latter case  $\omega_{\text{sky},1} + \omega_{\text{sky},2}$  would librate rather than  $\omega_{\text{sky},1} - \omega_{\text{sky},2}$  (39).

It is no coincidence that our six warm Jupiter systems are all characterized by mutual inclina-

tions abutting Kozai's minimum angle. In our regime in which the quadrupole potential still dominates and planetary eccentricities are low enough to avoid flips,  $39^\circ$  is the inclination that coincides with maximum eccentricity (minimum periape) and hence maximum tidal dissipation. Orbital decay during this maximum-eccentricity, minimum-inclination phase of the Kozai cycle naturally leads to an abundance of tidally migrated warm Jupiters with  $i_{\text{mut}}$  near  $39^\circ$  to  $65^\circ$  (48). The octupolar potential is not strong enough for our systems to alter this feature of quadrupolar Kozai cycles (6, 48). At the same time, the reason

why warm Jupiters have not completed their migration to become hot Jupiters is because of the special octupole-modified nature of their eccentricity variations. The usual (quadrupole) Kozai oscillations of eccentricity, which occur over the short nodal precession period, are modulated by an octupole-induced envelope (49) of much longer period following that of apsidal libration (Fig. 3 and figs. S1 to S5). The envelope period is approximately  $(a_2/a_1)(1 - e_2^2)/e_2$  longer than the Kozai time scale (46). This long-period modulation prevents eccentricities from surging too often and renders migration even slower than the "slow Kozai" migration described in (24). Such "super slow" evolution is similar to the "step" migration seen at high  $i_{\text{mut}}$  (6), except without the transition from prograde to retrograde orbital motion and the accompanying rapid tidal circularization. In the gentle and intermittent migration considered here, warm Jupiters reach the small periapees characterizing hot Jupiters only at the peaks of their eccentricity envelopes. As a proof of concept, we performed an integration of the secular equations of motion including tidal friction (Fig. 4). The warm Jupiter undergoes super slow tidal migration in which it librates apsidally and stalls in semimajor axis. A libration amplitude for  $\Delta\omega_{\text{inv}}$  near  $90^\circ$  enables super slow migration. If the libration amplitude were smaller, or if the apsidal separation were to circulate, then the envelope modulating the eccentricity would be less peaky, and the interior planet would spend more of its time near its maximum eccentricity. If the libration amplitude were larger, then not only would the apsidal separation be more prone to circulate given a small perturbation, but the system would also be more vulnerable to retrograde flips and concomitant eccentricity surges ( $e \rightarrow 1$ ). The upshot of all these scenarios (fig. S7) in which  $\Delta\omega_{\text{inv}}$  does not librate with an amplitude of  $90^\circ$  is that tidal migration, once begun, would rapidly complete and spawn a hot Jupiter.

The class of warm Jupiters we have identified is similar to the predicted class of Kozai-oscillating warm Jupiters (23), except that here the octupolar field generated by the eccentricity of the exterior perturber plays a starring role in effecting the observed near-orthogonality of periapee directions and in braking tidal migration. The mutual inclination of  $i_{\text{mut}} \sim 35^\circ$  to  $65^\circ$  that we have inferred from the measured apsidal misalignment attests to how the Kozai mechanism, working between planets, has indeed shaped planetary systems. Although large inclinations between hot Jupiters' orbital planes and the equatorial planes of their host stars are well established, our finding provides evidence that pairs of more-distant giant planets are themselves highly mutually inclined (although still prograde), in stark contrast to the flatness of solar system planets. The origin of such large inclinations is a mystery; planet-planet scattering (1) or secular chaos (2) are possibilities.

#### REFERENCES AND NOTES

1. F. A. Rasio, E. B. Ford, *Science* **274**, 954–956 (1996).
2. Y. Wu, Y. Lithwick, *Astrophys. J.* **735**, 109 (2011).
3. Y. Kozai, *Astron. J.* **67**, 591 (1962).
4. M. L. Lidov, *Planet. Space Sci.* **9**, 719–759 (1962).

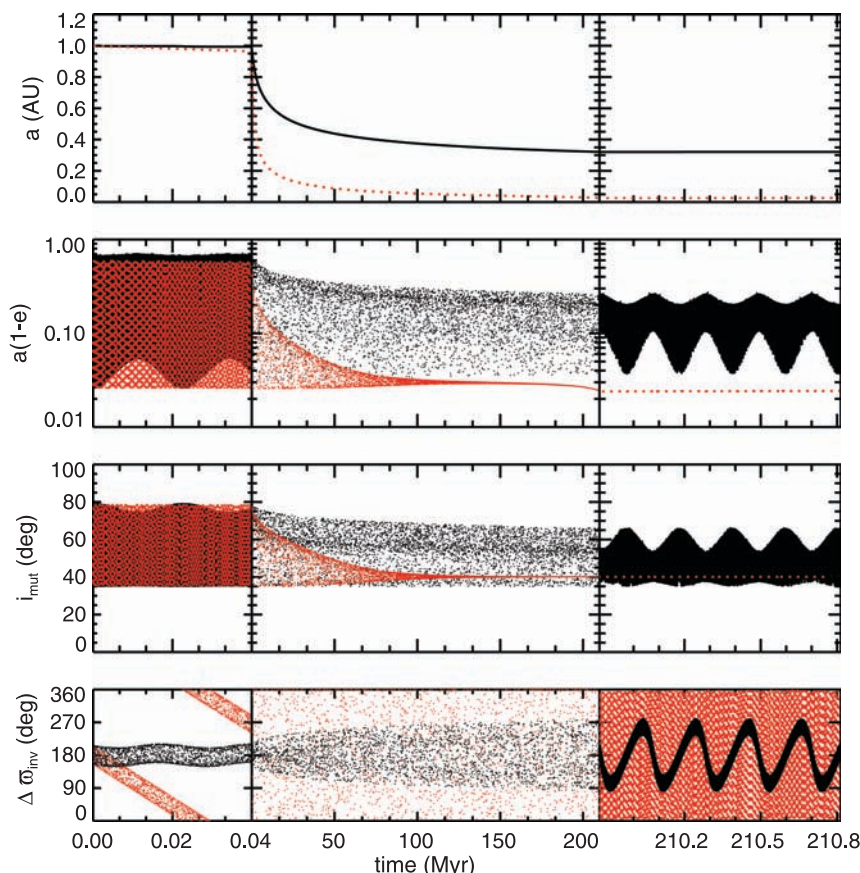


**Fig. 4. Tidal migration under a secular potential expanded beyond quadrupolar order can produce a stalled warm Jupiter.** Plotted are the time evolution of the inner planet's semimajor axis, periapee distance, mutual inclination with the outer planet, and apsidal separation, integrated using the test particle Hamiltonian expanded to hexadecapolar order (39); practically identical results are obtained with the octupolar Hamiltonian. Overplotted are results from the Hamiltonian including only up to quadrupolar terms (red dashed line) in which the inner planet fails to stall and instead becomes a hot Jupiter. General-relativistic precession is included for both planets (35). Tidal evolution was implemented using a constant tidal quality factor of  $10^5$ , a Love number of 0.26, and a planetary radius of 1 Jupiter radius (5). Tides raised on the star are not included because they are weak compared to tides raised on the planet at these semi-

major axes. The tidal forcing frequency is set to  $\sqrt{\frac{G(M_* + m_1)}{a_1(1 - e_1^2)}}$  (22). The outer planet has  $a_2 = 1.923$  AU,

$e_2 = 0.133$ , and  $m_2 = 6.59 M_{\text{Jupiter}}$ , matching HD 147018c, and initial  $\{i_2 = 0^\circ, \omega_2 = 17.2^\circ, \Omega_2 = 180^\circ\}$ . The inner planet (test particle) has initial  $a_1 = 1$  AU,  $e_1 = 0.9$ , and  $\{i_1 = 65^\circ, \omega_1 = 38.4^\circ, \Omega_1 = 0^\circ\}$ . With these choices, the eccentricity of the inner planet reaches a minimum of 0.33 at time = 220 years during the first Kozai cycle. The early tidal evolution, over the first ~20 million years, is subject to planet-planet scattering in a full  $N$ -body treatment; as such, the origin story portrayed in this figure is meant only to illustrate the concept of stalling, not to be definitive. This figure ends at ~200 million years, but similar histories spanning a few billion years are just as possible for different initial conditions or tidal efficiency factors.



5. Y. Wu, N. Murray, *Astrophys. J.* **589**, 605–614 (2003).
6. S. Naoz, W. M. Farr, Y. Lithwick, F. A. Rasio, J. Teyssandier, *Nature* **473**, 187–189 (2011).
7. G. Takeda, F. A. Rasio, *Astrophys. J.* **627**, 1001–1010 (2005).
8. M. Juric, S. Tremaine, *Astrophys. J.* **686**, 603–620 (2008).
9. D. Fabrycky, S. Tremaine, *Astrophys. J.* **669**, 1298–1315 (2007).
10. Y. Wu, N. W. Murray, J. M. Ramsahai, *Astrophys. J.* **670**, 820–825 (2007).
11. S. Chatterjee, E. B. Ford, S. Matsumura, F. A. Rasio, *Astrophys. J.* **686**, 580–602 (2008).
12. M. Nagasawa, S. Ida, *Astrophys. J.* **742**, 72 (2011).
13. T. D. Morton, J. A. Johnson, *Astrophys. J.* **738**, 170 (2011).
14. S. Naoz, W. M. Farr, F. A. Rasio, *Astrophys. J. Lett.* **754**, L36 (2012).
15. E. J. Rivera *et al.*, *Astrophys. J.* **719**, 890–899 (2010).
16. R. Sanchis-Ojeda *et al.*, *Nature* **487**, 449–453 (2012).
17. M. H. Lee, S. J. Peale, *Astrophys. J.* **567**, 596–609 (2002).
18. B. E. McArthur *et al.*, *Astrophys. J.* **715**, 1203–1220 (2010).
19. R. I. Dawson *et al.*, *Astrophys. J.* **71**, 89 (2014).
20. A. Cumming *et al.*, *Publ. Astron. Soc. Pac.* **120**, 531–554 (2008).
21. C. Petrovich, S. Tremaine, R. Rafikov, *Astrophys. J.* **786**, 101 (2014).
22. A. Socrates, B. Katz, S. Dong, <http://arxiv.org/abs/1209.5724> (2012).
23. S. Dong, B. Katz, A. Socrates, *Astrophys. J. Lett.* **781**, L5 (2014).
24. C. Petrovich, <http://arxiv.org/abs/1405.0280> (2014).
25. H. A. Knutson *et al.*, *Astrophys. J.* **785**, 126 (2014).
26. R. I. Dawson, R. A. Murray-Clay, *Astrophys. J. Lett.* **767**, L24 (2013).
27. E. I. Chiang, S. Tabachnik, S. Tremaine, *Astron. J.* **122**, 1607–1615 (2001).
28. T. A. Michtchenko, R. Malhotra, *Icarus* **168**, 237–248 (2004).
29. Queried from the Exoplanet Orbit Database (EOD) at [exoplanets.org](http://exoplanets.org) (50) on 8 April 2014.
30. Eccentricity was detected at two-sigma, and  $\Delta\omega_{\text{sky}}$  was detected with an uncertainty of  $<40^\circ$ .
31. We selected for eccentric warm Jupiters with only one known companion, because additional companions can disrupt Kozai oscillations. Our selection criterion thus excludes planetary pairs that are members of the 55 Cnc, epsilon Andromeda, mu Arae, HIP 14810, Kepler-9, and Kepler-30 systems. Moreover, each of these systems also has a close-in ( $a < 0.1$  AU) planet that would be disrupted if the warm Jupiter were to attain periape distances small enough for tidal circularization.
32. X. Tan *et al.*, *Astrophys. J.* **777**, 101 (2013).
33. For HD 202206c, modification of the semimajor axis from the best-fit value was required to avoid libration in the 5:1 resonance. See the supplementary materials for details.
34. J. E. Chambers, *Mon. Not. R. Astron. Soc.* **304**, 793–799 (1999).
35. D. C. Fabrycky, in *Exoplanets*, S. Seager, Ed. (Univ. of Arizona Press, Tucson, AZ, 2011), pp. 217–238.
36. D. Veras, E. B. Ford, *Astrophys. J.* **715**, 803–822 (2010).
37. A. L. Whipple, P. J. Shelus, *Icarus* **101**, 265–271 (1993).
38. J. Correa Otto, A. M. Leiva, C. A. Giuppone, C. Beaugé, *Mon. Not. R. Astron. Soc.* **402**, 1959–1968 (2010).
39. T. Yokoyama, M. T. Santos, G. Cardin, O. C. Winter, *Astron. Astrophys.* **401**, 763–772 (2003).
40. E. B. Ford, B. Kozinsky, F. A. Rasio, *Astrophys. J.* **535**, 385–401 (2000).
41. R. Barnes, R. Greenberg, *Astrophys. J. Lett.* **659**, L53–L56 (2007).
42. E. B. Ford, *IAU Symp.* **249**, 441–446 (2008).
43. B. Katz, S. Dong, R. Malhotra, *Phys. Rev. Lett.* **107**, 181101 (2011).
44. Y. Lithwick, S. Naoz, *Astrophys. J.* **742**, 94 (2011).
45. S. Naoz, W. M. Farr, Y. Lithwick, F. A. Rasio, J. Teyssandier, *Mon. Not. R. Astron. Soc.* **431**, 2155–2171 (2013).
46. G. Li, S. Naoz, B. Kocsis, A. Loeb, *Astrophys. J.* **785**, 116 (2014).
47. G. Li, S. Naoz, M. Holman, A. Loeb, *Astrophys. J.* **791**, 86 (2014).
48. L. G. Kiseleva, P. P. Eggleton, S. Mikkola, *Mon. Not. R. Astron. Soc.* **300**, 292–302 (1998).
49. The eccentricity of HD 202206b does not have such an envelope (fig. S5), which may be due to its proximity to the 5:1 mean-motion resonance and the large relative mass of the inner planet.
50. J. T. Wright *et al.*, *Publ. Astron. Soc. Pac.* **123**, 412–422 (2011).

51. Among the black diamonds, the planetary pairs with  $|\Delta\omega_{\text{sky}}|$  near  $90^\circ$  and large angular momentum ratios include giant planets in a five-planet system (55 Cnc), a pair of hot super-Earths (GJ 163), and a cold Jupiter partnered with a hot Neptune (HD 125612); it is unclear whether their orthogonal eccentricity vectors also signify large mutual inclinations. The transiting pair Kepler-30 c and d, which are near a 2:1 resonance, have  $|\Delta\omega_{\text{sky}}| = 114^\circ$ , an angular momentum ratio of 2:1, and a low mutual inclination (16°).

#### ACKNOWLEDGMENTS

We gratefully acknowledge support from the Miller Institute for Basic Research in Science, the University of California (UC) Berkeley's Center for Integrative Planetary Science, the National Science Foundation, and the National Aeronautics and Space Administration. This research has made use of the Exoplanet

Orbit Database at [exoplanets.org](http://exoplanets.org). This research employed the SAVIO computational cluster provided by the Berkeley Research Computing program, which is supported by UC Berkeley's Chancellor, Vice Chancellor for Research, and Chief Information Officer. We thank four anonymous referees for constructive feedback and D. Fabrycky and J. Johnson for helpful comments.

#### SUPPLEMENTARY MATERIALS

[www.sciencemag.org/content/346/6206/212/suppl/DC1](http://www.sciencemag.org/content/346/6206/212/suppl/DC1)  
Figs. S1 to S7

Table S1

References (52–63)

4 June 2014; accepted 12 September 2014

10.1126/science.1256943

#### EARLY UNIVERSE

## A local clue to the reionization of the universe

Sanchayeeta Borthakur,<sup>1\*</sup> Timothy M. Heckman,<sup>1</sup> Claus Leitherer,<sup>2</sup> Roderik A. Overzier<sup>3</sup>

Identifying the population of galaxies that was responsible for the reionization of the universe is a long-standing quest in astronomy. We present a possible local analog that has an escape fraction of ionizing flux of 21%. Our detection confirms the existence of gaps in the neutral gas enveloping the starburst region. The candidate contains a massive yet highly compact star-forming region. The gaps are most likely created by the unusually strong winds and intense ionizing radiation produced by this extreme object. Our study also validates the indirect technique of using the residual flux in saturated low-ionization interstellar absorption lines for identifying such leaky galaxies. Because direct detection of ionizing flux is impossible at the epoch of reionization, this represents a highly valuable technique for future studies.

The reionization of the universe is a crucial event in cosmic history. Identifying the source(s) responsible for reionization will allow us to understand the underlying physics. Star-forming galaxies are the most likely candidates, but what is their nature? By what process does Lyman continuum radiation, capable of ionizing hydrogen atoms, escape the region of dense and cold gas from which the required population of hot massive stars forms?

Studies to date have had limited success at detecting such candidates. For example, Iwata *et al.* (1) found continuum leaking out of 17 galaxies from their sample of 198 star-forming galaxies [Lyman break galaxies (LBGs) and Ly $\alpha$  emitters (LAEs)], whereas Vanzella *et al.* (2) found only one such leaking galaxy out of 102 LBGs. Most of the high-redshift studies have resulted in only a handful of detections with substantial escape fractions (3, 4). In some ways, the low incidence of such galaxies is not surprising. Hot massive stars are located in gas-rich regions with column densities ranging from  $10^{21}$  to  $10^{24}$  cm $^{-2}$ . This is 4 to

7 orders of magnitude higher than the column density of H I required to produce an optical depth of unity at the Lyman edge ( $N = 1.4 \times 10^{17}$  cm $^{-2}$ ). Therefore, extreme conditions may be required for a substantial fraction of the ionizing flux to escape from the galaxy.

Identifying local examples of such leaky galaxies will allow us to study in detail the processes that lead to the escape of Lyman continuum radiation. These local examples can also be used to validate indirect signatures of escaping ionizing flux that are based on the properties of the spectrum at wavelengths longer than the Lyman- $\alpha$  line (see below). This is invaluable, because the spectral region at shorter wavelengths is completely opaque at the epoch of recombination.

We previously uncovered a sample of relatively rare local (redshift  $z \approx 0.2$ ) starburst galaxies whose overall properties [mass, metallicity, size, morphology, star formation rate, kinematics, dust attenuation, etc.] are very similar to those of the LBGs (5–10). These galaxies are termed Lyman break analog galaxies (LBAs). SDSS J092159.38+450912.3 (hereafter J0921+4509) is one such local LBA ( $z = 0.23499$ ) that is producing stars at the rate of 50 solar masses ( $M_\odot$ ) per year. It belongs to a special class of LBA where several billion solar masses of stars are produced in an extremely compact central region with a radius of  $\sim 100$  pc (11). Such massive and highly

<sup>1</sup>Center for Astrophysical Sciences, Department of Physics and Astronomy, Johns Hopkins University, Baltimore, MD 21218, USA.

<sup>2</sup>Space Telescope Science Institute, 3700 San Martin Drive, Baltimore, MD 21218, USA. <sup>3</sup>Observatório Nacional, Ministry of Science, Technology, and Innovation, Rio de Janeiro, Brazil.

\*Corresponding author. E-mail: [sanch@pha.jhu.edu](mailto:sanch@pha.jhu.edu)